A Guha and J.B. Young, "Time-marching prediction of unsteady condensation phenomena due to supercritical heat addition",
In ***Turbomachinery : Latest Developments in a Changing Scene***, London, **IMechE**, 1991, p. 167-177.
(ISBN 0852987617)

C423/057

Time-marching prediction of unsteady condensation phenomena due to supercritical heat addition

A GUHA, BME, ME and J B YOUNG, MA, PhD
Whittle Laboratory, University of Cambridge

SYNOPSIS An unsteady one dimensional time-marching technique has been developed that can be employed for any type of wet steam flow : nucleating or non-nucleating, subcritical or supercritical, steady or unsteady. It is robust, accurate, simple and fast. The scheme uses a novel technique that performs the integration of the droplet growth equations along the fluid path lines rather than the more usual method which involves freezing the gas dynamic flowfield instantaneously in order to perform the integration. This allows simultaneous solution of all the relevant equations and thus the correct coupling between the vapour-phase gasdynamics and the relaxation effects due to the droplets is maintained. The scheme maintains a polydispersed droplet spectrum which is essential for modelling the nucleation zone accurately. Calculations based on the present scheme show good agreement with experimental measurements, steady and unsteady, reported in the literature.

It is also shown how the unsteady condensation process due to supercritical heat addition may give rise to a polydispersed droplet spectrum. This has a direct bearing on a possible explanation of the poly-dispersity measured in steam turbines ; a polydispersity which cannot be predicted with existing steady flow calculation methods.

1 INTRODUCTION

The homogeneous condensation of pure steam in converging-diverging nozzles can result in both steady and unsteady modes of operation depending on the inlet stagnation conditions of the steam. In the periodically unsteady mode of operation, the inlet stagnation state is close to dry saturated and homogeneous nucleation occurs in the transonic region just after the nozzle throat. The resultant heat release causes a compressive wave to develop of such a strength that a steady operating position cannot be found. The wave therefore propagates towards the nozzle throat, the subsequent pressure rise causing a reduction in nucleation rate and hence heat release rate. With the cause of its inception removed, the strength of the wave decreases and the flow again expands through the throat in a shock free manner thus allowing the whole process to repeat itself.

Such types of instability due to supercritical heat addition were first reported by Schmidt (1962), for the case of humid air. High speed photography revealed the existence of moving shock waves. Quantitative experiments were then conducted by Barschdorff (1967,1970) both for humid air and pure steam. He investigated two different nozzle shapes and measured frequencies from 500 to 1000 Hz. In an attempt to correlate the experimental measurements, Zierep and Lin (1968) derived a similarity law to express the dimensionless frequencies of the unsteady flow within certain ranges of nozzle geometries and supply conditions. Wegener and Cagliostro (1973) also carried out an experimental study of unsteady moist air flows in nozzles using a special short-duration supersonic wind tunnel, called a Ludwieg tube. This provided a well-controlled flow that permitted operation with increased relative humidities and pressures as well as variable supply temperatures. In this way, the range of frequency measurement was extended to about 6000 Hz. They also carried out a dimensional analysis applicable to arbitrary supply conditions and cooling rates at the nozzle throat. However, data near the condition of incipient unsteady flow and from one of the nozzles of Barschdorff (1970), which had a low cooling rate, could not be correlated on a universal plot of dimensionless frequency versus relative humidity. This implied that the empirical relation is only valid for a limited range of nozzle shape and supply conditions and in cases where the unsteady flow is well established.

Barschdorff and Filippov (1970) analyzed pressure and density data, calculated shock positions in the nozzle, and presented an approximate method for calculating the frequency of oscillation. However, as noted by Wegener and Cagliostro (1973), solutions of the full equations of motion in conjunction with a rate equation for heat addition by condensation are required for a full understanding. Since it is not possible to solve the unsteady equations analytically, it is necessary to resort to numerical calculations. Recently, Skillings and Jackson (1987) have reported a time-marching technique based on the MacCormack explicit scheme, which is capable of dealing with unsteady nucleating flow. The scheme generates 'ripples' before and after the shock wave, however, and the solution procedure involves decoupling between the phases which results in, to quote the authors, "a diminished ability to predict unsteady flows". The gas field is effectively fixed instantaneously in a pseudo-steady state whilst the droplet growth integrations are performed.

In this paper, we describe a robust, one dimensional time-marching technique that can be employed for any type of wet steam flow : nucleating or non-nucleating, subcritical or supercritical, steady or unsteady flow. The scheme uses a novel technique that performs the integration of the droplet growth equations along the fluid *path lines* rather than the usual, quasi-unsteady, method of integration described above*. This allows simultaneous solution of all the relevant equations and enforces the correct coupling between the vapour-phase gasdynamics and the relaxation effects due to the presence of the liquid phase. The scheme also allows retention of a polydispersed droplet spectrum (unlike most existing one- and two- dimensional computer programs) which is essential for modelling the nucleation zone accurately. Calculations based on the present scheme show much closer agreement with experimental measurements reported in the literature.

* The term "path line" is used in its usual formal sense to describe the locus of the position of a specified fluid particle on a time-distance diagram. In the Skillings and Jackson method, the pressure field was frozen at a given instant of time while the growth of the liquid phase was calculated. This technique does not model the true unsteady flow correctly.

2 GOVERNING EQUATIONS

Wet steam is assumed to be a homogeneous mixture of vapour, at pressure p and temperature T_g, and spherical droplets of various sizes. The continuous distribution of droplets is discretized into a number of groups such that the i^{th} group contains n_i droplets per unit mass of mixture of radius r_i and mass m_i. The wetness fraction y_i is then the sum of contributions from all groups and is given by:

$$y = \Sigma y_i = \Sigma n_i m_i \qquad (1)$$

If the vapour density is ρ_g, the mixture density (neglecting the volume of the liquid phase) is :

$$\rho = \rho_g / (1-y) \qquad (2)$$

and the mixture specific enthalpy is :

$$h = (1-y) h_g + \Sigma y_i h_i \qquad (3)$$

where h_g and h_i are the specific enthalpies of the vapour phase and i^{th} group of droplets respectively.

For sub-micron size particles the slip velocity between the two phases may be neglected. Therefore, only thermal non-equilibrium i.e. differences in the temperatures of the two phases will be considered here. Under such circumstances the gas dynamic equations for inviscid adiabatic unsteady two-phase flow can be written as :

Continuity $$\frac{\partial \rho}{\partial t} + \nabla.(\rho \underline{V}) = 0 \qquad (4)$$

Momentum $$\frac{\partial \underline{V}}{\partial t} + (\underline{V}.\nabla)\underline{V} + \frac{\nabla p}{\rho} = 0 \qquad (5)$$

Energy $$\frac{\partial}{\partial t}\left[\rho\left(e + \frac{V^2}{2}\right)\right] + \nabla.\left[\rho \underline{V}\left(h + \frac{V^2}{2}\right)\right] = 0 \qquad (6)$$

where $\underline{V}$ is the common velocity of the two phases and e is the specific internal energy of the mixture.

Equations (4) - (6) are identical to those describing the adiabatic flow of an inviscid single phase fluid. The differences are apparent, however, when it is recalled that the wetness fraction y in equations (2) and (3) is not necessarily the equilibrium value and that h_g and h_i in equation (3) are evaluated at temperatures T_g and T_i which are not necessarily equal to the local saturation value T_s.

2.1 Nucleation rate

The nucleation rate equation employed in the present work is that described by Frenkel [see McDonald (1962-63) for a full derivation] and later corrected by Kantrowitz for non-isothermal effects [see Young (1982)]. The rate of nucleation of embryonic droplets per unit volume, J, is thus given by

$$J = \frac{1}{1+\phi} q_c \sqrt{\frac{2\sigma}{\pi m^3}} \cdot \frac{\rho_g^2}{\rho_l} \cdot \exp\left(-\frac{4\pi r^{*2}\sigma}{3kT_g}\right) \qquad (7)$$

where σ is the surface tension, ρ_l is the liquid density, m is the mass of a molecule, k is Boltzmann's constant, q_c is the condensation coefficient and the non-isothermal correction factor ϕ is given by

$$\phi = \frac{2(\gamma - 1)}{\gamma + 1} \frac{h_{fg}}{R_g T_g}\left(\frac{h_{fg}}{R_g T_g} - \frac{1}{2}\right)$$

where h_{fg} is the specific enthalpy of evaporation, R_g is the specific gas constant and γ is the ratio of specific heat capacities.

The critical radius r* is expressed as :

$$r^* = \frac{2\sigma T_s}{\rho_l h_{fg} \Delta T} \qquad (8)$$

where ΔT, the degree of supercooling, is defined as $\Delta T = T_s(p) - T_g$, where $T_s(p)$ is the saturation temperature corresponding to pressure p. Many studies have established the basic correctness of this nucleation rate equation, although modifications to improve the accuracy are still being suggested.

2.2 Growth of the liquid phase

As a result of the high latent heat of water, the growth rate of liquid droplets in pure steam is limited not by the rate at which vapour can reach the surface, but by the rate at which heat can be conducted away from the droplet. The generally accepted form of the droplet growth equation, valid over a wide range of pressures and flow regimes (from free-molecule to continuum), is that of Gyarmathy (1963). However, in order to predict droplet radii which agree well with experimental measurements, Young (1982) found that, in the low pressure range, a higher growth rate than that prescribed by Gyarmathy is necessary. He, therefore, postulated that, under non-equilibrium conditions when net condensation is occurring, the evaporation coefficient q_e falls below the condensation coefficient q_c. Their relation to each other was determined by introducing a droplet growth parameter α, the value of which lay between 0 and 9, depending on the prevailing pressure. Including this effect the droplet growth equation takes the revised form:

$$(h_g - h_i)\frac{Dr_i}{Dt} = \frac{\lambda_g (T_i - T_g)}{r_i \rho_l \left(\frac{1}{1+4Kn_i} + 3.78(1-\nu)\frac{Kn_i}{Pr_g}\right)} \qquad (9)$$

where λ_g and Pr_g are the thermal conductivity and Prandtl number of the vapour phase respectively and Kn_i is the Knudsen number of the droplets in the i^{th} group given by : $Kn_i = l_g / 2r_i$, l_g being the mean free path of a vapour molecule. ν is given by

$$\nu = \frac{R_g T_s(p)}{h_{fg}}\left[\alpha - \frac{1}{2} - \frac{2-q_c}{2q_c}\left(\frac{\gamma+1}{2\gamma}\right) c_p \frac{T_s(p)}{h_{fg}}\right] \qquad (10)$$

where c_p is the specific heat capacity of the vapour.

It is worth mentioning here that if one considers the net bulk velocity of the gas molecules towards the droplet surface when condensation is occurring (the Schrage effect) then the mass transfer equation for the droplets gets multiplied by the factor $2q_c/(2-q_c)$. The value of the Schrage correction factor becomes 2 if one assumes the value of the condensation coefficient to be unity. This has prompted researchers to introduce the correction factor 2 into the energy transfer equation also and this has the effect of doubling the droplet growth rate. However, if one carries out the kinetic theory calculation meticulously it is found that the Schrage effect has a negligible effect on the energy transfer between the two phases and hardly influences the droplet growth rate at all.

(The very small impact of the Schrage effect on the droplet growth rate can be readily appreciated by examining the expression for ν given above.) Thus, for example, the factor Sc in the expression for α_j in the paper by Skillings and Jackson(1987) is found to be an artificial factor designed to double the droplet growth rate and is actually without any physical basis whatsoever.

The growth rate of the liquid phase can be related to the growth rate of individual droplets through equation (1). Noting that the mass of a droplet of the i^{th} group is given by :

$$m_i = 4/3\ \pi\, r_i^3\, \rho_l \qquad (11)$$

it follows that :

$$\frac{Dy}{Dt} = \sum \frac{Dy_i}{Dt} = \sum \frac{3y_i}{r_i}\frac{Dr_i}{Dt} \qquad (12)$$

where the differentiation with respect to time is the substantive derivative, i.e. $\frac{D}{Dt} = \frac{\partial}{\partial t} + \underline{V}.\nabla$.

[Note that, for the existing droplets, the n_i 's do not change, because velocity slip between the two phases is assumed to be negligible.]

By combining a mass transfer equation with Eqn (10), Gyarmathy also showed that, to a good approximation, the phase temperature difference is given by :

$$T_i - T_g = \Delta T - \Delta T_{cap,i} \qquad (13)$$

where $\Delta T_{cap,i}$ is the capillary supercooling of the droplet given by :

$$\Delta T_{cap,i} = \frac{2\sigma_i T_s}{\rho_l r_i h_{fg}} \qquad (14)$$

σ_i being the surface tension of the liquid at temperature T_i. It is convenient to define a *thermal relaxation time* by :

$$\tau_{T,i} = \frac{(1-y)\, c_p r_i^2 \rho_l \left(\frac{1}{1+4Kn_i} + 3.78\,(1-\nu)\frac{Kn_i}{Pr_g}\right)}{3\,\lambda_g\, y_i} \qquad (15)$$

Substituting Eqns. (9) , (13) and (15) into Eqn (12) gives :

$$(h_g - h_i)\frac{Dy_i}{Dt} = \frac{(1-y)\, c_p\, (\Delta T - \Delta T_{cap,i})}{\tau_{T,i}} \qquad (16)$$

Eqn (16) shows that the time rate of change of y_i following a given fluid particle is directly proportional to the excess of the vapour supercooling above the liquid capillary supercooling and is inversely proportional to the thermal relaxation time.

2.3 Thermal Non-Equilibrium

The secret of obtaining quantitative information about wet steam flows is to obtain the variation of supercooling through the expansion. Once this is known, all other variables can be calculated comparatively easily. Normally the complete system of gasdynamics and droplet growth equations are solved numerically, but this can be a time-consuming business, especially for a polydispersed flow with a large number of droplet groups. A much simpler, semi-analytical procedure is, however, possible under certain circumstances (Young , 1984). Taking the scalar product of the momentum Eqn (5) with $\underline{V}$ and combining Eqn (4) and Eqn (6) in the usual way gives :

$$\frac{Dh}{Dt} = \frac{1}{\rho}\frac{Dp}{Dt} \qquad (17)$$

Introducing Eqn (3), the droplet growth Eqn (16) , the Clausius-Clapeyron Equation and standard thermodynamic relationships gives, after considerable algebraic manipulation,

$$\frac{D(\Delta T)}{Dt} + \frac{(\Delta T - \Delta T_{cap})}{\tau_T} = F\frac{Dln(p)}{Dt} \qquad (18)$$

where, $F = \frac{p}{(1-y)c_p\rho_s}\left(\frac{cT_s}{h_{fg}} - (1-y)(\alpha_t T_g)\frac{\rho_s}{\rho_g}\right)$ (19)

c being the specific heat of the mixture,

$$c = (1-y)\, c_p + \Sigma\, y_i\, c_i \qquad (20)$$

α_t is the coefficient of thermal expansion and for an ideal gas $\alpha_t T_g = 1$. Calculations presented in this paper assume that the vapour is a semi-perfect gas with heat capacities as functions of the temperature only. τ_T and ΔT_{cap} are the thermal relaxation time and the capillary supercooling applicable to the droplet spectrum as a whole and given by :

$$\frac{1}{\tau_T} = \sum \frac{1}{\tau_{T,i}} \qquad (21)$$

$$\Delta T_{cap} = \sum \frac{\tau_T}{\tau_{T,i}}\,\Delta T_{cap,i} \qquad (22)$$

Apart from very minor approximations, Eqn (18) is an exact first order differential equation for the variation with time of supercooling of a fluid particle and is valid for the general case of unsteady, three dimensional flow. F is a function predominantly of the saturation conditions and its variation with pressure is very small. It is to be noted that the contribution of freshly nucleated droplets has not been taken into account in the above equation (for the computational domain over which they have been nucleated). However, because of their extremely small size, they account for a very small proportion by mass of the liquid phase and the latent heat released during their formation is also, correspondingly, small.

For values of τ_T which are small compared with the flow transit time, Eqn (18) is the archetype of a mathematically stiff differential equation. In these circumstances numerical integration procedures using conventional finite differencing would lead to unstable amplification of error unless very small time increments were employed. One strategy to avoid this problem is to integrate Eqn (18) analytically over time increments such that τ_T, ΔT_{cap} and F Dln(p) / Dt remain approximately constant. As τ_T changes only slowly through an expansion, the size of increments is then dictated by the rate of change of flow properties rather than by the relaxation time. Applying this technique, the integration of Eqn (18) gives,

$$\Delta T = \Delta T_0\, e^{-t/\tau_T} + \tau_T\left(F\dot{P} + \frac{\Delta T_{cap}}{\tau_T}\right)\left(1 - e^{-t/\tau_T}\right) \qquad (23)$$

where ΔT_0 is the supercooling at the start of the time increment and $\dot{P}$ is the expansion rate defined by Dln(p) / Dt. The above semi-analytical method was suggested by Young(1984) and can be extended to calculate the wetness fractions by substituting Eqn (23) into Eqn (16) and integrating the resulting equations in the same manner. The result is :

$$y_i = y_{io} - \frac{(1-y)\, c_p\, \Delta T_{cap,i}}{h_{fg}\, \tau_{T,i}}\, t + \frac{(1-y) c_p \tau_T}{h_{fg} \tau_{T,i}} \cdot \left[(\Delta T_o - \Delta T) + \left\{ F\dot{P} + \frac{\Delta T_{cap}}{\tau_T} \right\} t \right] \qquad (24)$$

3 DEVELOPMENT OF A 'COMPUTATIONAL, WET-STEAM BLACK-BOX'

It has already been shown that, if velocity slip is neglected, the continuity, momentum and energy equations for the two-phase, vapour-droplet flow become identical with their single-phase counterparts if the mixture density ρ and specific enthalpy h are used throughout. In this situation, the thermodynamics of the problem can be almost completely uncoupled from the gas dynamics. At any particular stage of the iterative solution procedure, the current solution of the gas dynamic equations provides a pressure distribution for input to the thermodynamic routines which, in turn, provide updated values of mixture density and specific enthalpy for inclusion in subsequent iterations of the gas dynamic routines. The overwhelming advantage of this approach is that the computational section dealing with the thermodynamic aspects is self-contained and can be easily coupled with single-phase calculation schemes for the gas dynamics which are already available.

Our objective, therefore, is to develop computer subroutines for evaluating the thermodynamic equations (23) and (24) for a given time increment over which the expansion rate $\dot{P}$ is specified. At the start of the time increment the state of the steam is completely specified by the pressure and vapour supercooling, together with the droplet radius and wetness fraction associated with each liquid group present. The necessary calculations are then performed to evaluate the vapour supercooling and droplet spectrum at the end of the time-interval. We refer to these subroutines as a 'computational, wet-steam black-box' and the mode of operation is illustrated in Fig. (1).

For implementing this scheme, three different situations have been recognized :

(1) Dry superheated or supercooled steam : This case arises when the wetness fraction is zero and the nucleation rate is less than a specified minimum value. (In this work, nucleation is neglected if $J<10^{15}$ nuclei / m^3.s, as below this value nucleation will have a negligible effect on the flow behaviour.) In this case calculation is straight-forward. The change in supercooling is obtained from the equation :

$$\frac{D(\Delta T)}{Dt} = \left[\frac{T_s}{\rho_s h_{fg}} - \frac{1}{c_p \rho_g} - \frac{1-\alpha_t T_g}{c_p \rho_s} \right] \frac{Dp}{Dt}$$

and there is no need to calculate the droplet spectrum. It should be noted that negative ΔT means that the vapour is superheated.

(2) Wet Non-Nucleating Flow : This corresponds to the case when the wetness fraction is greater than zero but the nucleation rate is less than the specified minimum. In this case the supercooling is determined by Eqn (23) and the wetness fractions are calculated from Eqn (24). Since the flow is non-nucleating, the droplet number per unit mass in each group is conserved. From the computed wetness fractions and droplet numbers, the radii of the droplets can be found from the relationship $y_i = n_i m_i$. Note that, in the case of polydispersed flow, Eqn (24) represents a set of equations, one for each droplet group. However, all the common terms and those properties which do not change appreciably have been grouped suitably and are calculated once only so that the computational time for n droplet groups is considerably less than n times the computational time for a single group.

(3) Nucleating Flow : In this case the nucleation rate is greater than the specified minimum limit. Therefore, side by side with the growth of existing droplets, if any, new droplets of size r^* [given by Eqn (8)] are nucleated at the rate J [given by Eqn (7)]. Since the droplets grow rapidly, the thermal relaxation time may vary considerably over these time increments. Thus, the integrated forms of supercooling and droplet growth equations [Eqns (23) and (24)] , which assume a constant thermal relaxation time, are not used. Instead, Eqns (18) and (9) are solved simultaneously by a Fourth-order Runge-Kutta scheme. At the end of the time increment a new droplet group consisting of those droplets nucleated during the interval, is added.

Calculations in nucleating regions of the flow are more time consuming than those in non-nucleating regions where the integrated form of equations is applicable. Also, since a new droplet group is nucleated over each time increment, the number of droplet groups may become computationally unmanageable. To alleviate this problem, a scheme has been developed whereby droplet groups containing droplets of approximately the same radius are merged into a single group. However, a sufficient number of droplet groups (typically 8-10) is always retained so that the accuracy of the solution is not degraded. In this way the approximate shape of the droplet spectrum is maintained without consuming excessive CPU time or computer memory.

4 COUPLING OF THE 'WET-STEAM BLACK-BOX' WITH A TIME-MARCHING METHOD FOR SOLVING THE GAS DYNAMIC EQUATIONS

The 'wet-steam black-box' described in the previous section can be used independently only if the local expansion rate is prescribed. However, in general, the pressure distribution specifying this parameter must be obtained from a solution of the gas dynamic equations. For the calculations described in this paper, the black-box was coupled to a one-dimensional time-marching procedure similar to that which had been used successfully for single-phase calculations.

Time dependent solutions of the Euler equations are now widely used for the analysis of the flow through turbomachinery blade rows. Their main attraction is their ability to compute mixed subsonic-supersonic flows with automatic capturing of shock waves. Since the droplet growth laws are more easily applicable to individual fluid particles, a mixed Eulerian-Lagrangian technique is used for the present work. In this technique, the continuity and momentum equations are solved in their usual Eulerian forms. However, the energy equation in the Euler solver is effectively substituted by the wet-steam black-box, thermodynamic calculation* . At the end of a particular computational time-step, the continuity and momentum equations furnish updated values of density and velocity respectively. The wet-steam black-box gives the vapour temperature T_g (via the supercooling) and all the wetness parameters. Finally, the equation of state for the vapour gives an updated value of the pressure. One is then ready to repeat the same calculation procedures for the next computational element and so on.

The unsteady Eulerian flow equations for a one-dimensional co-ordinate system applied, in integral form, to a control volume ΔV over a time step Δt are as follows :

* A rather similar procedure is often used for computing isentropic flows of a perfect gas when the energy equation is replaced by the condition of constant entropy along fluid path lines.

Continuity $\Delta\rho = \Sigma(\rho V_x dY)\,\Delta t / \Delta V$

Momentum $\Delta(\rho V_x) = \Sigma(p + \rho V_x^2)dY\,\Delta t / \Delta V$

where V_x is the flow velocity.

The Time-marching scheme employed is similar to that of Denton(1983). The finite volume elements are formed such that the grid points are at the faces of the control volumes.The fluxes of mass and momentum through each face are then found from the flow properties stored at the grid points. These fluxes may then be used in the RHS of the continuity and momentum equations to obtain the changes in ρ and V_x for the element in time Δt. All the changes in flow properties are then applied to the downstream node of the element.

Since the aim was to develop a scheme that would be applicable to all flow regimes including steady and unsteady supercritical regimes where shock waves are present, it was found necessary to apply an explicit artificial viscosity in the form of a pressure correction term in the momentum equation. For this purpose, instead of using the correct value of the pressure at the grid point concerned, a slightly downwinded value is used for calculating the pressure force term in the momentum equation. For a smoothly varying flow this introduces negligible error.

At the inlet boundary, constant stagnation pressure and temperature are specified. At the outlet boundary, static pressure is specified only if the flow is subsonic.

Since the time-marching procedure is an explicit method, it has to satisfy the Courant-Friedrich-Lewy (CFL) criterion of stability. The CFL criterion determines the maximum stable time step Δt as:

$$\Delta t < \frac{\Delta x}{(V_x + a)}$$

where Δx is the axial distance between two adjacent grid points and a is the local sound velocity. In practice Δt is taken as $\Delta t = TF\ \Delta x / (V_x + a)$, where TF is an arbitrary factor to ensure stability which, from experience, lies in the range 0.1 to 0.7.

5 RESULTS AND DISCUSSION

The main implication of supersaturation is that when steam expands through a nozzle, droplets do not appear as soon as the condition line crosses the saturation line. For some considerable time after this point the steam remains dry in a metastable equilibrium until the supersaturation ratio becomes high enough to trigger an appreciable nucleation rate. The droplets thus formed then grow in size by exchanging heat and mass with the surrounding vapour. If the flow velocity in the nucleation zone is supersonic, the heat released by the growing droplets causes a gradual increase in pressure known, somewhat inaptly, as the 'condensation shock'.

For high initial superheat at nozzle inlet, the 'condensation shock' occurs in the diverging section of the nozzle. Inside the condensation zone the effect of heat addition overrides that of area change and so the flow velocity decreases but always remains above the local sonic speed. Downstream of the condensation zone the area change becomes dominant and the Mach number (the flow being still supersonic) starts increasing again. This is the regime of so called subcritical heat addition. Figure (2) shows the prediction of the computer program in such a situation for two different inlet conditions. The nozzle profile used was that of Moses and Stein (1978). For experiment 257, the superheat at the stagnation condition is 14.5 K ; while, for experiment 258, the corresponding quantity is 16.6 K. Both the predicted pressure profile and mean droplet radius agree very well with the experimental measurements. It is to be stressed here that such an agreement cannot be made simply by modifying the nucleation equation and retaining Gyarmathy's growth model without including the parameter α of Eqn (10). For a discussion on this topic the reader is referred to the paper by Young (1982).

As the initial superheat is reduced, the steam attains the saturation condition earlier in the nozzle and consequently the condensation shock appears closer to the throat (Fig. 2). The pressure rise becomes steeper and the Mach number at the end of the condensation zone is closer to unity. For one particular inlet superheat the Mach number at the end of the condensation zone is exactly equal to unity and the flow is said to be thermally choked. It is to be noted that the flow then passes through two sonic points - one at the throat (corresponding to conventional aerodynamic choking) and one at the end of the condensation zone. This condition represents the critical amount of heat that the flow can absorb while maintaining a continuous variation of flow parameters. If the amount of heat liberated exceeds this critical quantity then no continuous solution of the gasdynamic equations is possible, although a steady state may be obtained by the formation of a steep fronted shock wave inside the condensation zone. In this case the flow passes the sonic point at the throat, becomes supersonic in the diverging section, decelerates somewhat due to partial condensation and recompresses through an aerodynamic shock wave. The resulting subsonic flow then accelerates to the sonic speed due to the remaining rapid condensation and finally accelerates supersonically due to increase of area. Figure (3) shows one such case of steady supercritical heat addition . The nozzle depicted is that of Moore et. al (1973) and the prediction corresponds to the test marked E_2 in Skillings and Jackson (1987). The initial superheat in this case is ~5 K. The calculated droplet size agrees well with the measurements. The predicted pressure rise at the shock is greater than that indicated experimentally, and the pressure then decreases slightly faster than do the measurements.

If the inlet superheat is reduced further, the aerodynamic shock wave forms nearer the throat and becomes stronger. At some point the strength of the shock demanded by the heat release that accelerates the flow to the sonic condition becomes higher than that which the local flow velocity can sustain and the shock becomes unstable. This gives rise to an oscillatory flow pattern where the shock wave moves upstream while a new one develops somewhere downstream. Such unsteady flow generally occurs when T_0 (the inlet stagnation temperature) is near the saturation temperature corresponding to p_0 (the inlet total pressure). Figure(4) shows the computational prediction in such a situation. The test case corresponds to Test 4 in Skillings et. al. (1987). The pressure profiles at different instants during a complete cycle reveal exactly the same sequence of the formation and movement of the shock wave as explained above. According to the predictions the shock weakens as it approaches the throat and, in fact, becomes of negligible strength a little upstream of the throat. Thus a self-excited oscillating flow results, which arises purely because of the dynamics of the flow, the nozzle geometry being fixed and the inlet boundary conditions remaining steady. If attention is focussed on the time history of the static pressure at a point 20 mm downstream of the throat for the example chosen, the pressure variation shown in Figure(5) results. It can be seen that the variation is periodic with a frequency of about 540 Hz and an amplitude of about 24.5 mbar. The experimental values measured at the same location were ~400 Hz and ~20 mbar respectively.

Considering the complications of predicting the movement of shock waves even in single phase flows, the agreement between the theoretical computation and the experiment is quite good. It is also gratifying, from the computational point of view, to find that the calculation converges to the periodic solution with very little delay after

the wet steam routines were introduced (see Fig. 5). (Due to the large variation in flow properties during the initial time-marching iterations it is not advisable to call the wet steam subroutines until some degree of convergence of the vapour flowfield has been obtained.) Since different schemes to accelerate the convergence (for example, the use of 'local time-steps', 'multi-grids', etc.) that are very useful in steady-flow calculations, are unsuitable for unsteady predictions, the CPU time required is higher in the latter case. The calculations were performed using a single processor of an Alliant FX-80 computer and the CPU time required to compute the unsteady flow shown in Figures 4 and 5 was approximately 2 minutes per one complete cycle of oscillation. However, it should be mentioned that the computer program has not yet been tried to be fully optimized and appreciable reduction in the CPU time may be achieved by utilizing further vectorization of the code.

The solid line in Figure(5) shows the time history of the variation of pressure at the same point using a pseudo-unsteady scheme similar to that of Skillings et al (1987). Since, in the pseudo-unsteady scheme, the gas-field is effectively frozen while the droplets are allowed to propagate down the nozzle, the downstream points feel the influence of the upstream aerodynamic shock-wave too early. The new shock wave therefore develops earlier and the whole process repeats within a shorter period of time leading to a higher computed frequency. Thus, the present full unsteady scheme predicts a frequency of ~540 Hz in comparison to that of ~650 Hz predicted by the pseudo-unsteady scheme. While the predicted frequency in the former case is still higher than the measured value, the change is in the right direction.

Figure (6) shows a comparison of the prediction with the experiments conducted by Barschdorff (1970). The frequencies of oscillation for Barschdorff's nozzle-I have been calculated using the present code for different inlet conditions and are compared with the experimental values. It can be seen that the frequency increases with decreasing inlet stagnation temperature. This can be explained by recalling that, with decreased inlet stagnation temperature, the shock wave will initially be formed closer to the throat and the two extreme positions, at which it will have negligible effect on the nucleation, will move closer together. Thus, the whole process of the formation, upstream movement and weakening of the shock wave to the point where the compression has a negligible effect on the condensation process, repeats faster, giving rise to a higher frequency. Once again, the predicted frequencies are higher than the measured values, although the correct trend is reproduced. It is to be noted that, since the frequency decreases very rapidly with increase of inlet stagnation temperature until the oscillation dies away completely, a small error in the temperature measurement would shift the experimental curve substantially. This, together with the uncertainties in the nucleation rate equation, the droplet growth laws and a possible boundary layer / shock wave interaction in a sensitive area like the vicinity of the throat may be responsible for the differences in measured and predicted frequencies of oscillation.

An interesting implication of the unsteady nucleation process is that it may explain, to some extent at least, the nature of the phase change occurring in a real steam turbine. The measured droplet size distribution in a turbine is normally polydispersed and highly skewed with a Sauter mean diameter in the range 0.2 - 0.6 μm (Walters, 1980). Conventional nucleation calculations linked to a steady-flow gas dynamic analysis generally predict Sauter mean diameters of the order of 0.1 μm or less with very small polydispersity. (In fact, most existing calculation methods treat the droplet population as monodispersed and are not suitable for the prediction of flows characterized by strong liquid polydispersity.) Thus, although these calculation methods (which agree reasonably well with steady-flow experiments in one-dimensional nozzles) can sometimes predict the peak of the droplet size distribution measured in turbines, it is not yet established from where the larger droplets constituting the "tail" of the distribution originate. It is, however, of crucial importance to understand the mechanism of formation of such a droplet spectrum, as such an understanding would elucidate, at least indirectly, the fluid mechanics of the wet steam flow through a turbine and would allow the determination of the other important effect of wetness, namely the loss of turbine efficiency associated with the liquid phase.

The possible occurrence of unsteady nucleation processes in turbines may shed some light on the origins of the measured polydispersed spectra. Figure(7) shows the variation of the Sauter mean diameter at the nozzle exit corresponding to the unsteady pressure fluctuation shown in Figure(5). It can be seen that the mean radius changes by a factor of three (from ~0.06 μm to ~0.18 μm) during one period of the oscillation. The reason for the existence of such a broad band of droplet sizes is that, as the aerodynamic shock wave moves upstream towards the throat and interacts with the nucleation zone, progressively fewer droplets are nucleated thus resulting in a larger final mean radius. Considering any particular cycle and constructing the average droplet spectrum over that cycle (number density of droplets versus droplet radius), then the curve shown in Figure(8) is obtained. A probe, located at the exit of the nozzle for sufficient duration of time, would register such a droplet size distribution. The calculated spectrum is significantly polydispersed, highly skewed and bears the same qualitative features as those measured in turbines. In a transonic turbine blade passage, it is thought that the condensation process may often occur near the throat where there is the possibility of an interaction with the shock-wave system generated by the trailing edge flow. Such an unsteady interaction was indeed observed by Skillings et. al. (1988), although it must be stated that a possible explanation of the unsteadiness was not the condensation process itself but was instead fluctuations in the free shear layer boundaries extending downstream of the cascade. The expansion rate in a turbine is generally less than that in most laboratory nozzle experiments and hence the mean droplet size in a turbine is likely to be higher than that in the calculation described above. However, whether or not this can account for mean droplet diameters of the order of 0.5 μm, as measured in turbines, remains to be investigated.

6 CONCLUSION

A robust one-dimensional unsteady time-marching method has been developed that can be used for any flow regime encountered in wet steam. It is accurate, simple and fast. The wet-steam black-box developed can also be used in isolation if the expansion rate is prescribed and can easily be incorporated in different, established single phase calculation procedures. The predicted frequencies of unsteady oscillation are in better agreement with experiments than those obtained from pseudo-unsteady calculations. The computer program models correctly all the basic physics of the unsteady condensation process, for example, the increase in frequency of oscillation with decrease of inlet stagnation temperature. It has been shown that a poly-dispersed droplet spectrum results from such unsteady processes. Similar unsteady processes resulting from the interaction of the condensation zone with the oblique shock waves at the trailing edge in a turbine blade passage may be responsible, to some extent, for the observed polydispersity in the droplet-size spectra measured in real turbines.

ACKNOWLEDGEMENT The work was performed at the Whittle Laboratory and A. Guha was supported by The Prince of Wales Scholarship from Trinity College.

REFERENCES

1 Barschdorff D., 'Droplet Formation, Influence of Shock Waves and Instationary Flow Patterns by Condensation Phenomena at Supersonic Speeds', Proceedings of the Third International Conference on Rain Erosion and Associated Phenomena, Elvatham Hall, New Hampshire, England, 1970, p 691.

2 Barschdorff D., 'Stromungsmechanik und Stromungsmaschinen', Verlag G. Braun, Karlsruhe, 1967, vol. 6, p 18.

3 Barschdorff D. and Filippov G. A., 'Analysis of Certain Special Operating Modes of Laval Nozzles with Local Heat Supply', Heat Transfer - Soviet Research, 1970, vol. 2, No. 5, p 76.

4 Denton J.D., 'An Improved Time-Marching Method for Turbomachinery Flow Calculation', Trans. A.S.M.E. (J. Eng. for Power), 1983, vol. 105, p 514.

5 Guha A., 'The Fluid Mechanics of Two-phase Vapour-droplet Flow with Application to Steam Turbines", PhD dissertation submitted to the University of Cambridge, 1990.

6 Gyarmathy G., Z. angew Math. Phys., 1963, vol.14, no. 3, p 280.

7 McDonald J.E., 'Homogeneous Nucleation of Vapour Condensation', Am.J.Phys., 1962-3, vol. 130, pt. 1, p 870, vol. 31, pt. 2, p 31.

8 Moore M.J., Walters P.T., Crane R.I. and Davidson B.J., 'Predicting the Fog-drop Size in Wet-Steam Turbines', Inst. Mech. Engrs., Wet Steam 4 Conference, Paper C/37/73, 1973.

9 Moses C.A. and Stein G.D., 'On the Growth of Steam Droplets Formed in a Laval Nozzle using both Static Pressure and Light Scattering Measurements', ASME J. Fluids Eng., 1978, vol. 100, p 311.

10 Schmidt B., Jahrbuch WGLR, 1962, p 160.

11 Sichel M., 'Unsteady Transonic Nozzle Flow with Heat Addition', AIAA, 1981, vol. 19, no. 2, p 165.

12 Skillings S.A. and Jackson R., 'A Robust Time-Marching Solver for One-dimensional Nucleating Steam Flows', Heat and Fluid Flow, 1987, vol. 8, no. 2, p 139.

13 Skillings S.A. ,Walters P.T. and Moore M.J., 'A Study of Supercritical Heat Addition as a Potential Loss Mechanism in Condensing Steam Turbines', IMechE Conference, Cambridge, England, 1987, paper C259/87, p 125.

14 Skillings S.A., 'A reconsideration of Wetness Loss in LP Steam Turbines', Proc. BNES Conf. on 'Technology of Turbine Plant Operating with Wet Steam', London, 1988, p 171.

15 Walters P.T., 'Practical Application of Inverting Spectral Turbidity Data to Provide Aerosol Size Distribution', Applied Optics, 1980, vol. 19, p 2353.

16 Wegener P.P. and Cagliostro D.J., 'Periodic Nozzle Flow with Heat Addition',Combustion Sc. and Technology, 1973, vol. 6, p 269.

17 Wegener P.P. and Mosnier F., 'Periodic Transonic Flow with Heat Addition: New Results', Combustion Sc. and Technology, 1981, vol. 24, p 179.

18 Young J.B., 'Semi-analytical Techniques for Investigating Thermal Non-equilibrium Effects in Wet Steam Turbines', Int. J. Heat and Fluid Flow, 1984, vol. 5, no. 2, p 81.

19 Young J.B., 'The Spontaneous Condensation of Steam in Supersonic Nozzles', PhysicoChemical Hydrodynamics, 1982, vol. 3, no. 1, p 57.

20 Zierep J. and Lin S. Forsch. Ing. Wes., 1968, vol. 34, no. 4, p 97.

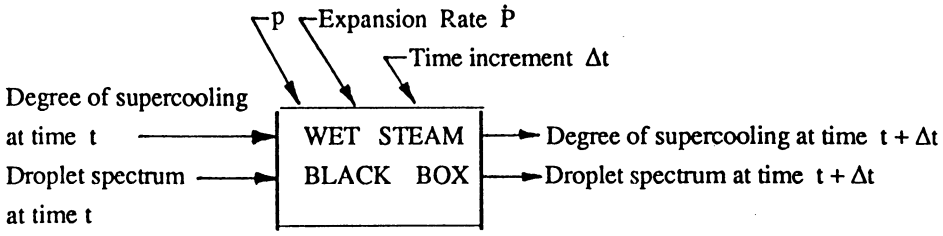

Fig 1 Block diagram of the wet steam black-box

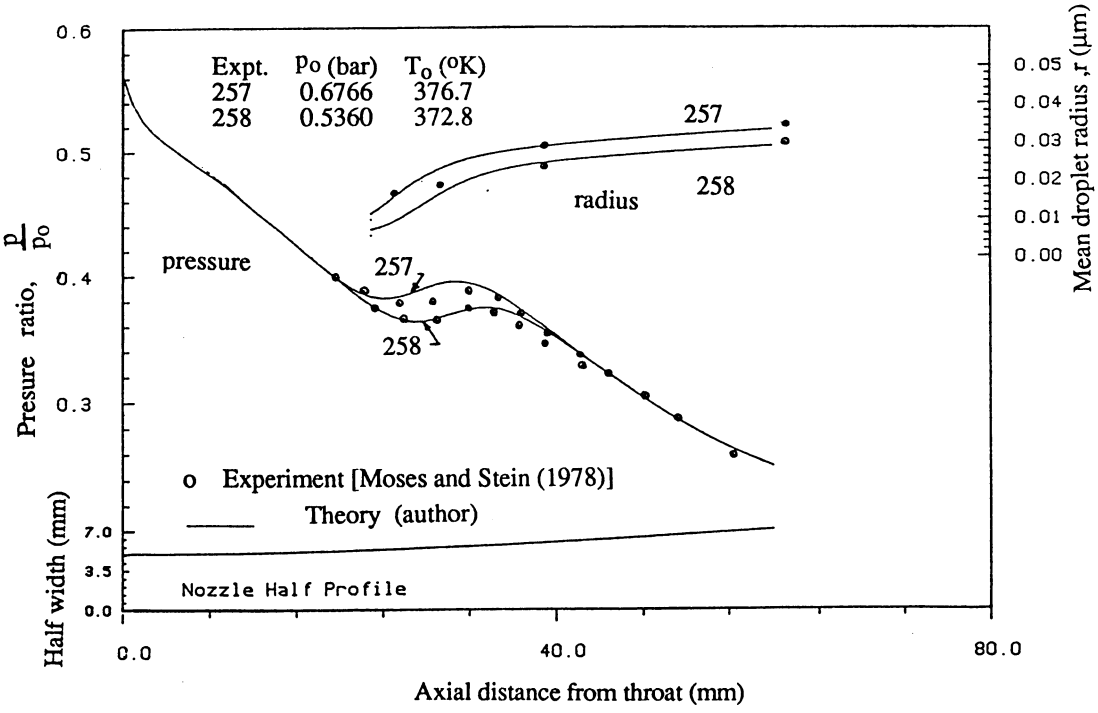

Fig 2 Subcritical heat addition: comparison of theory with experiments

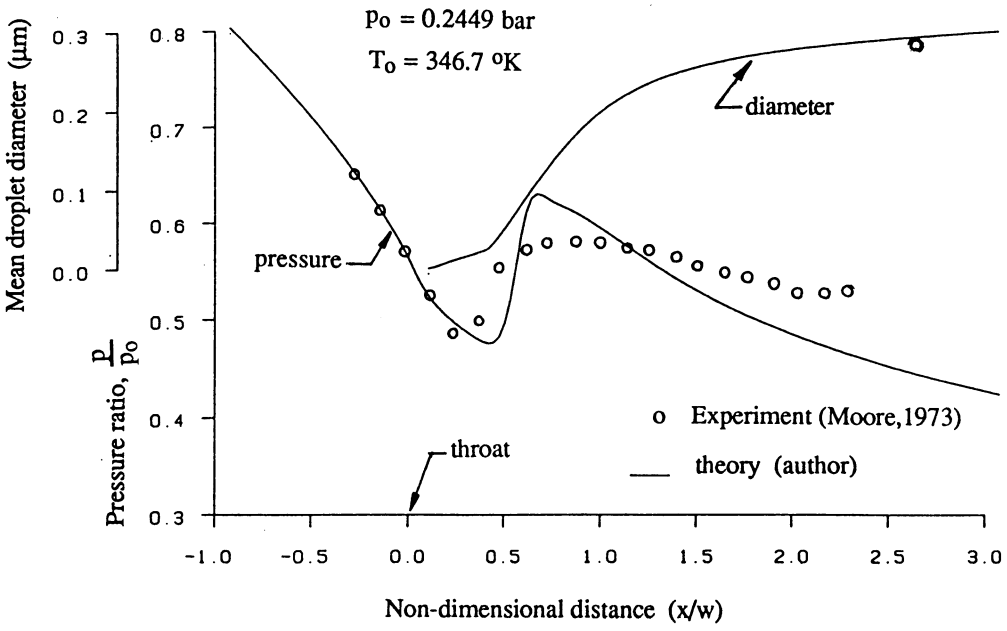

Fig 3 Steady supercritical heat addition: comparison of theory with experiment

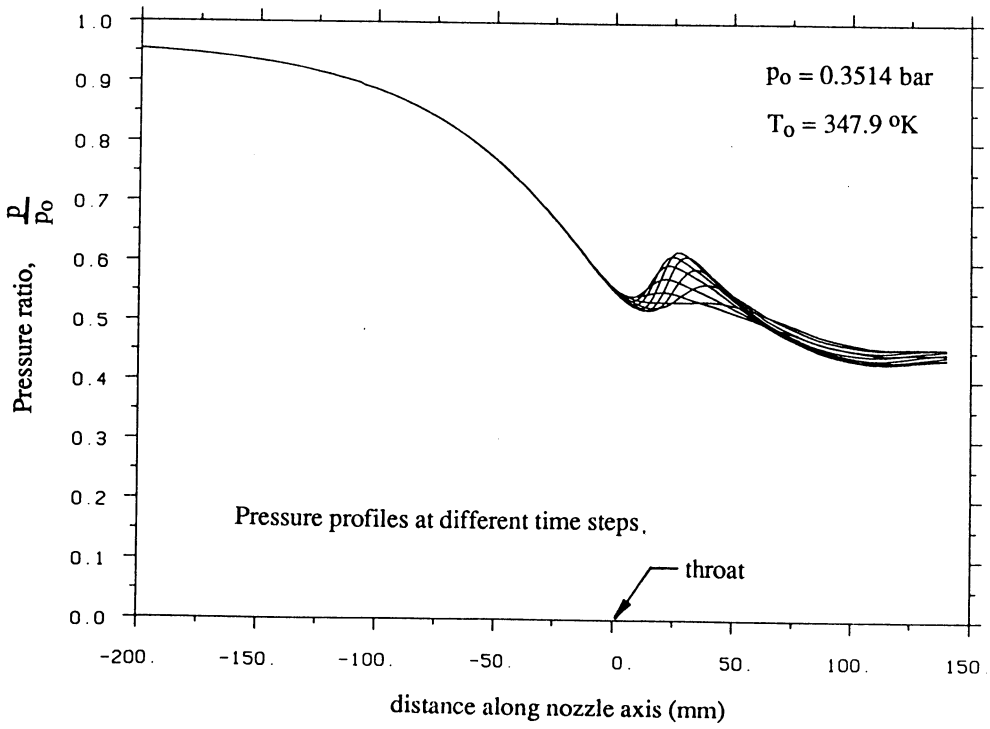

Fig 4 Unsteady supercritical heat addition: evolution of pressure profiles for one cycle

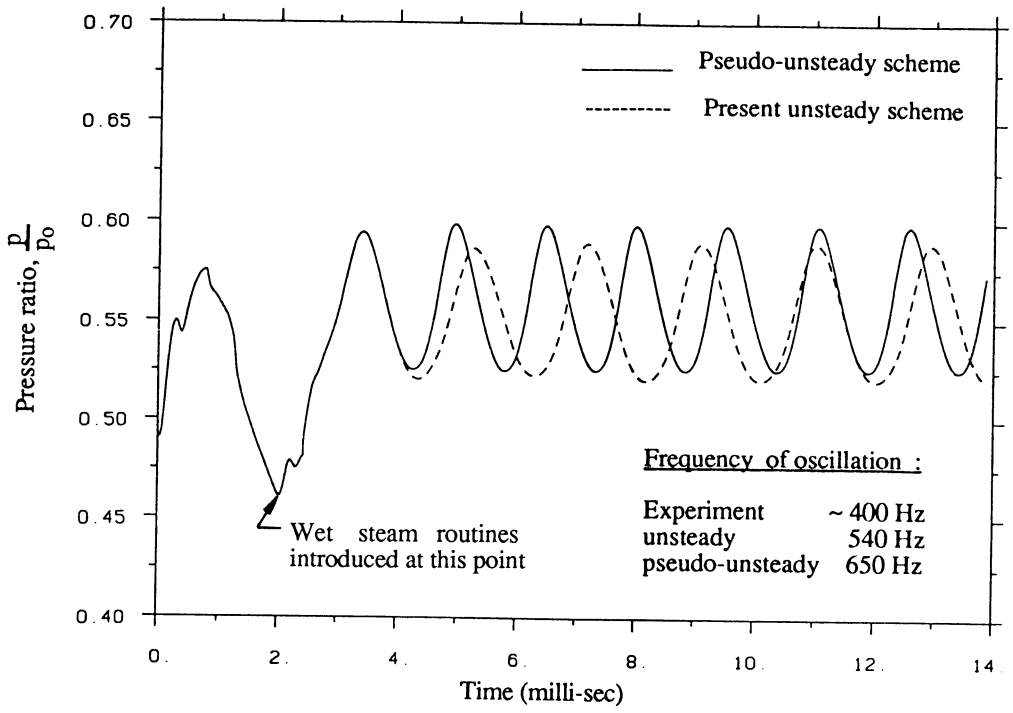

Fig 5 Variation of pressure at a point near throat: comparison of different unsteady schemes

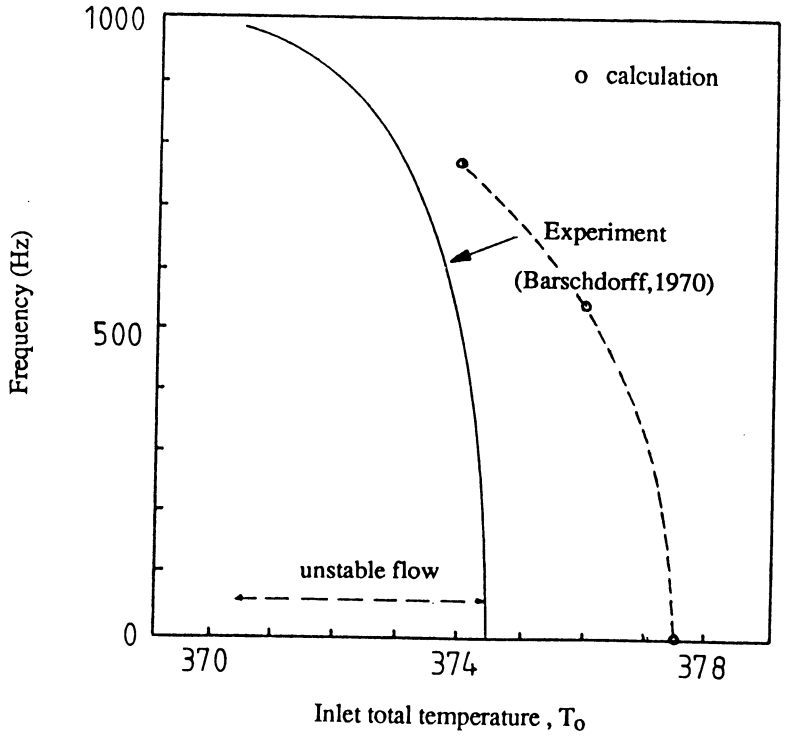

Fig 6 Variation of frequency of oscillation with T_o : comparison of experiment and computation

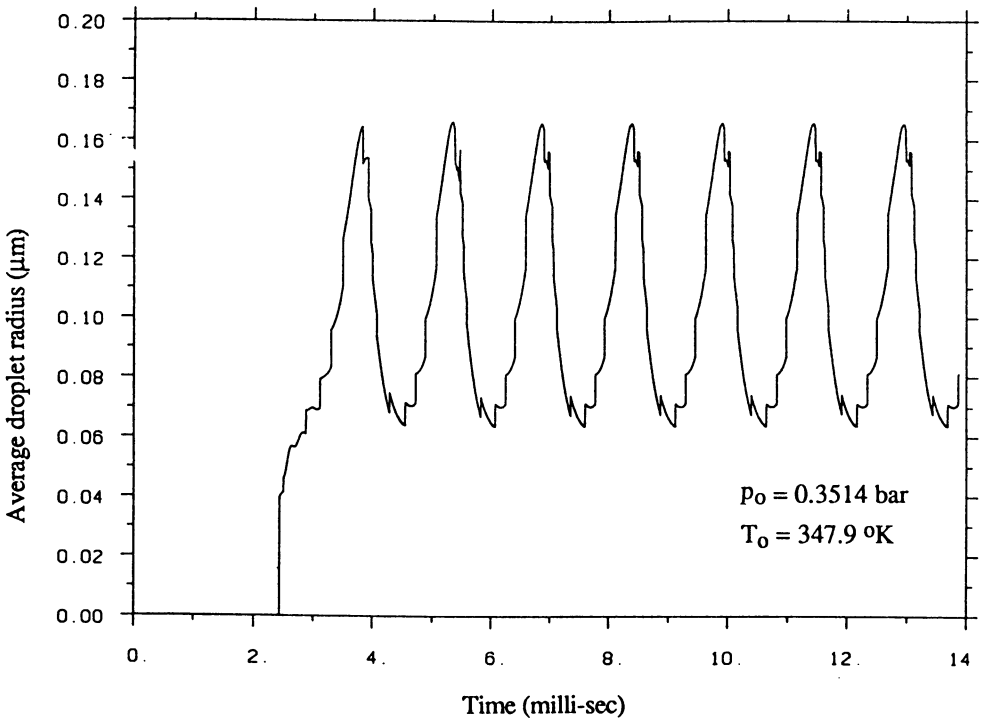

Fig 7 Variation of the average droplet radius at nozzle exit: unsteady flow corresponding to Fig 5

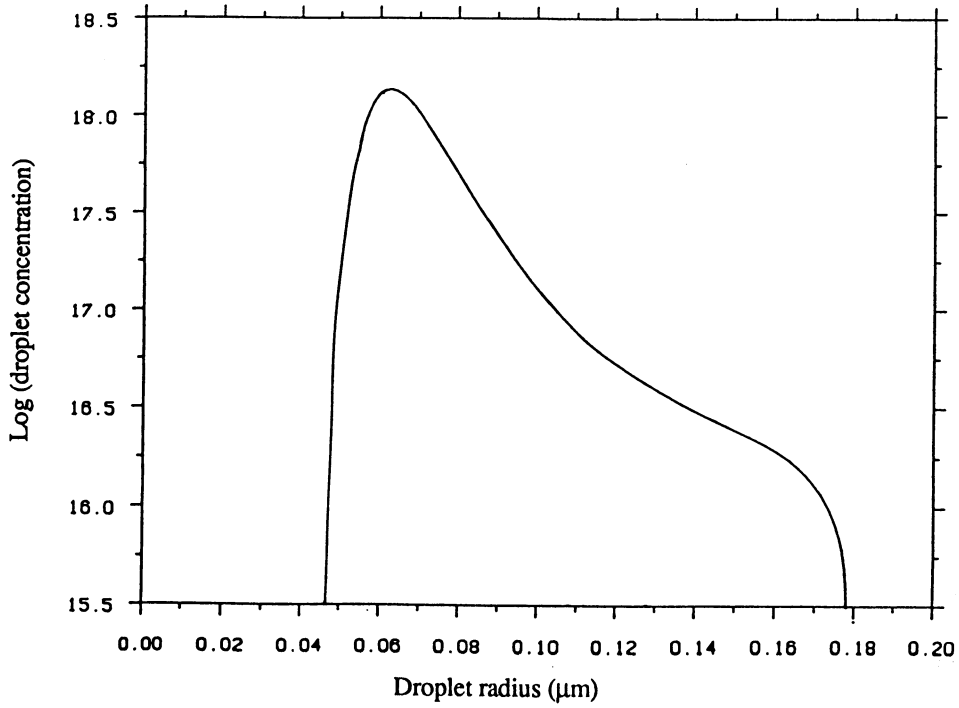

Fig 8 Droplet spectrum at nozzle exit